Int J Thermophys (2014) 35:2124–2139
DOI 10.1007/s10765-014-1715-0

Analog Front-End Circuitry in Piezoelectric and Microphone Detection of Photoacoustic Signals

Tomasz Starecki

Received: 21 April 2014 / Accepted: 1 August 2014 / Published online: 24 August 2014

Abstract This paper is a review of analog front-end circuitry used in photoacoustic equipment with microphone or piezoelectric detection. A block structure of the front end as well as detailed circuit diagrams of preamplifiers dedicated for piezoelectric sensors and measurement condenser and electret microphones are described. The presented circuits are optimized toward low-noise operation. Practical remarks regarding the design of the remaining analog blocks are also given. The analysis shows that it is possible to design an analog front end for which specifications will be comparable with the best commercial solutions.

Keywords Analog front-end · Condenser microphone · Electret microphone · Low-noise preamplifiers · Photoacoustic equipment · Piezoelectric sensor

1 Introduction

There are many kinds of detectors used in photoacoustic equipment [1–18]. Some of them are quite sophisticated solutions—e.g., optical microphones [6,7], quartz resonator-based detectors [13–15], and microcantilevers for which the deflection is measured with interferometric techniques [16–18]. Such solutions are typically aimed at increases of the sensitivity of the detector, but usually they are associated with high complexity and cost. Quite often they are also patented, which prevents their wider use, particularly in commercial applications. As a result, a great part of practical implementations of photoacoustic equipment still uses detectors much simpler, and

T. Starecki (✉)
Institute of Electronic Systems, Warsaw University of Technology, Nowowiejska 15/19, 00-665 Warsaw, Poland
e-mail: tomasz@starecki.com; t.starecki@ise.pw.edu.pl

thus much cheaper and easier to use, based on piezoelectric transducers [9–11] or microphones [1–4].

Selection of a detector used in a particular application depends strongly on the physical state and form of the substance under investigation. Piezoelectric transducers are used mainly in photoacoustics of liquids [19–22] and solids for which the forms allow for direct contact with the transducer [23–26]—e.g., semiconductor structures [25,26]. They are also commonly used in medical and imaging applications [27,28], as well as for the study of nanoparticle suspensions [29,30]. Microphones are applied mainly in photoacoustic investigations of gases [1,2,31–34] and such solids in which piezoelectric detection would be difficult—e.g., powders [35,36].

In a laboratory environment, processing of the output signals from such sensors is typically performed by means of specialized equipment, i.e., dedicated preamplifiers, amplifiers, synchronous detectors, etc. It should be noted, however, that the development of an analog front end dedicated for photoacoustic measurements is relatively easy. And such a design can have technical specifications comparable to characteristics of the mentioned specialized equipment, at many times lower cost, size, power consumption, etc. As a result, it is possible to develop a relatively simple, but very convenient tool for use in photoacoustic experiments in laboratory conditions, as well as in the field. This paper discusses basic issues regarding the design of such an analog front-end circuitry dedicated for photoacoustic detection with piezoelectric sensors or microphones.

2 Analog Front-End Block Structure

A typical block structure of the analog front end with photoacoustic detection performed by means of a microphone or piezoelectric sensor is presented in Fig. 1. The main components of such a structure are

- input transducer, i.e., microphone or piezoelectric sensor, which converts pressure changes in the photoacoustic cell into electrical signals,
- preamplifier,
- amplifying-filtering block,

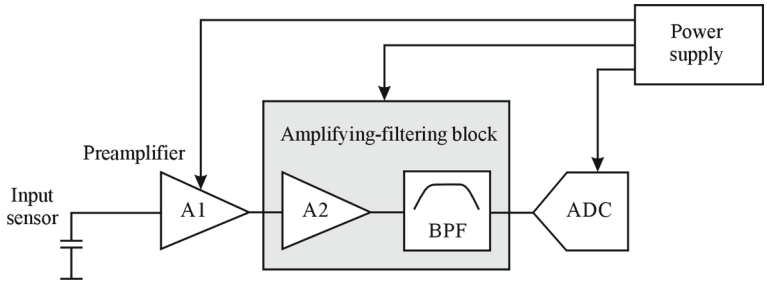

Fig. 1 Block diagram of an analog front end dedicated for piezoelectric and microphone detection of photoacoustic signals

- analog-to-digital converter, and
- power supply.

Design and specifications of the mentioned components should be adjusted to the target application and properties of the input sensor.

3 Input Sensor

As already mentioned, the most common photoacoustic signal detectors (input sensors) are microphones and piezoelectric transducers. Knowledge of their properties is very important, as these properties have direct impact on the characteristics of the photoacoustic instrument and also result in some requirements regarding design of the next stage of the signal path.

3.1 Piezoelectric Transducers

Operation of all piezoelectric transducers is based on a piezoelectric effect. This phenomenon is observed when a mechanical deformation of a piezoelectric material produces a change in the electric polarization of that material, i.e., electric charge appears on certain opposite faces of the piezoelectric material when it is mechanically loaded [37,38]. Properties of piezoelectric materials are defined by means of several parameters, among others, by a piezoelectric charge constant (d) and piezoelectric voltage constant (g). The piezoelectric charge constant is defined as the electric polarization generated in a material per unit of mechanical stress applied to this material, while the piezoelectric voltage constant is defined as the electric field produced in a material per applied unit of mechanical stress. It should be noted that some piezoelectric materials may have a high charge constant and a moderate voltage constant, while other materials may have a higher voltage constant and a moderate charge constant. This means that piezoelectric materials can be divided into two basic kinds: capacitive and charge emitting. Examples of charge-emitting sensors are commonly used PZT piezoceramics, which have a high charge sensitivity of 580 $\mathrm{pC{\cdot}N^{-1}}$ and a moderate voltage constant 38 $\mathrm{V{\cdot}m{\cdot}N^{-1}}$, while quartz, which in turn has a low charge sensitivity of 4.6 $\mathrm{pC{\cdot}N^{-1}}$ (charge constant) but a relatively high voltage sensitivity of 118 $\mathrm{V{\cdot}m{\cdot}N^{-1}}$ [39], can be an example of a capacitive material. All the piezoelectric materials are high-impedance signal sources and thus require an appropriate design of the following stage (preamplifier).

3.2 Microphones

The microphones which are most commonly used in photoacoustic applications are

- Measurement condenser microphones [40,41],
- Measurement electret (pre-polarized condenser) microphones [41,42],
- Low-cost electret microphones [43,44], and
- MEMS microphones [44–48].

Operation of all these kinds of microphones is based on deflection of a conductive plane (usually a membrane) which results in changing of the sensor capacitance according to the applied pressure changes.

Measurement condenser and electret microphones have usually a form close to a cylinder for which the diameter is 1/8 in (3 mm), 1/4 in (6 mm), 1/2 in (13 mm), or 1 in (25 mm) [40–42]. In photoacoustic applications, the most common are 1/2 in (13 mm) microphones dedicated for pressure measurements. The sensitivity of such microphones is typically not more than 50 $\mathrm{mV{\cdot}Pa^{-1}}$ (sensitivity of 1/4″ (6 mm) microphones is typically at the level of 1.6 $\mathrm{mV{\cdot}Pa^{-1}}$) [40–42]. The influence of the temperature, humidity, static pressure, and aging on the sensitivity is so low that they can be neglected. These microphones also have a very high dynamic range (over 140 dB) and low noise, which is typically at the level of 1.1 $\mathrm{\mu Pa{\cdot}Hz^{-1/2}}$ for 1/2 in (13 mm) microphones [40,42]. Unfortunately, their prices are relatively high (start at about $1000), which prevents them from use in many general-purpose lower cost applications. The capacitance of such microphones is typically a few to a few tens of picofarads [40,42], which at lower acoustic frequencies corresponds to the impedance at the level of GΩ. Thus, a high-impedance input preamplifier must be used with such sensors. An additional requirement in the case of measurement condenser microphones is +200 V DC polarization voltage.

In many applications, an alternative for measurement microphones is low-cost, electret microphones (typical price range of $1 to $10) dedicated for consumer applications or for use in hearing instruments [43,44]. Their most common sizes are in the range of 3 mm to 6 mm, offering a typical sensitivity below 10 $\mathrm{mV{\cdot}Pa^{-1}}$ [43,44]. These microphones have a low-impedance output (typically a few kΩ) due to an internal FET-based voltage follower, which simplifies design of the following stages, but their dynamic range is low and the stability is poor. Additional problems result from a moderate or even poor signal-to-noise ratio and power supply rejection ratio (PSRR) [43,44].

An even better sensor can be found among commercially available MEMS microphones, which have a higher sensitivity (10 $\mathrm{mV{\cdot}Pa^{-1}}$ to 100 $\mathrm{mV{\cdot}Pa^{-1}}$) at a similar or even lower price ($1 to $5), a smaller size—typically, 1.85 mm × 2.75 mm to 3.8 mm × 4.7 mm (L × W), and a moderate dynamic range and stability [44–48]. Similar to the low-cost electret microphones, they are equipped with an internal voltage follower/amplifier, and offer a moderate or poor S/N and PSRR. Some MEMS microphones models have direct digital output, usually I2S (e.g., ICS-43430 and ADMP441ACEZ), or PDM interface (e.g., WM7210, SPK0415HM4H-B, AKU440, and INMP522), and their use in photoacoustics has already been reported [49]. However, taking into consideration that the photoacoustic signal is usually relatively low and requires substantial amplification, voltage output microphones are more suitable in such applications. Although the above specifications may not seem yet particularly impressive, it should be mentioned that some papers have reported MEMS microphones of much better characteristics—e.g., sensitivity over 2000 $\mathrm{mV{\cdot}Pa^{-1}}$, at dimensions less than 3 mm × 3 mm [50], which clearly shows that there is a lot of room for improvement, and further strong progress in the field of MEMS microphones should be expected.

4 Preamplifier

The main role of a preamplifier used in photoacoustic equipment with a microphone or piezoelectric detection is conversion of the input signal available at a high-impedance output of the sensor to a low-impedance (not more than a few kΩ, preferably less than 100 Ω) signal source. The preamplifier stage should also be optimized toward the lowest possible noise. Amplification of the signal is desired, but not critical, as it can be done in the following stages, which work at a low signal source impedance, so that it can be quite easily designed with very low inherent noise. In the case of a piezoelectric sensor, the two basic preamplifier configurations are a voltage follower (Fig. 2a) and charge amplifier (Fig. 2b) [38,51–54]. The basic preamplifier circuits for condenser and electret (pre-polarized) microphones are given in Figs. 2c and d [55,56].

4.1 Voltage Amplifier for Piezoelectric Sensors

In the voltage follower circuit (Fig. 2a), the output of the operational amplifier follows the voltage from the non-inverting input, which means that the circuit should be used with capacitive transducers (which have a higher voltage constant), rather than with charge-emitting ones. The resistor R is required to supply a bias current to the non-inverting input of the amplifier. The resistive component of the sensor impedance is very high, so that $R \ll R1$ even if R is in the range of GΩ. Noise analysis of such a voltage follower can be based on the circuit diagram presented in Fig. 3, where i_n and u_n are, respectively, the current noise and voltage noise of the operational amplifier, while u_{nR} is the noise of resistor R. Taking into consideration that the noise voltage increases with the resistance, it may seem at first glance that R should be reduced to

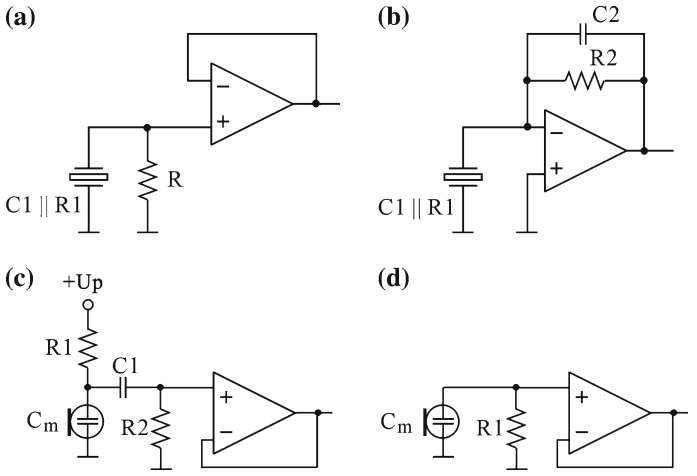

Fig. 2 Basic structure of preamplifiers dedicated for capacitive transducers: (a) voltage amplifier for piezoelectric sensor, (b) charge amplifier for piezoelectric sensor, (c) preamplifier for measurement condenser microphone, and (d) preamplifier for measurement electret microphone

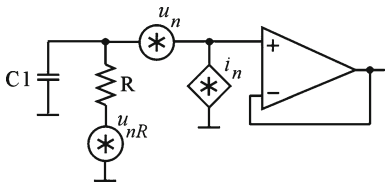

Fig. 3 Circuit diagrams used for noise analysis of the input stage of the preamplifier from Fig. 2a

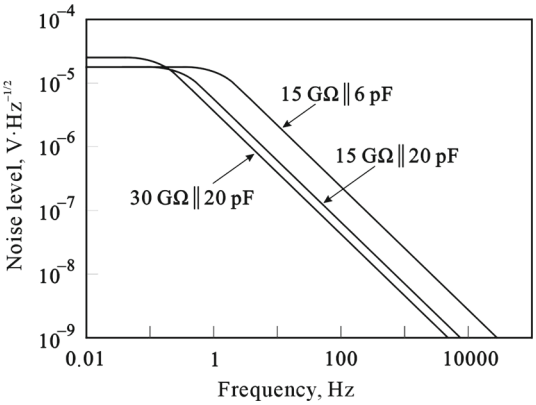

Fig. 4 Influence of the input resistance on the noise properties of the preamplifier [55]

such a value, and that the lower cutoff frequency of the amplifier (resulting from the time constant defined by the R and $C1$ values) is equal or slightly below the lowest frequency used in the measurements. But it should be noted that connection of the R and $C1$ acts as a high-pass filter with respect to the signal to be measured, while it acts as a low-pass filter with respect to the noise generated by the resistance. And, while the time constant of the mentioned low-pass filter is proportional to the resistance, the noise voltage increases with the square root of the resistance value. As a result, noise properties of the amplifier should improve with the input resistance value (Fig. 4) [55]. Therefore, it is convenient to have R as large as possible.

Taking into consideration that the input bias current I_B of the amplifier passes through R resulting in an additional input offset voltage, the operational amplifier should be a CMOS or JFET with possibly the lowest i_n and u_n noise values. A practical example of a preamplifier for a piezoelectric sensor working in the voltage mode is shown in Fig. 5. The operational amplifier used in the presented solution is LMC662, for which typical specifications are $I_B = 2$ fA, $u_n = 22$ nV·Hz$^{-1/2}$, and $i_n = 0.2$ fA·Hz$^{-1/2}$. The amplifier works with a gain of $K = 1 + R2/R3$ (which for the component values as given in Fig. 5 is approximately 10). Such an approach has two main advantages over a simple voltage follower. First, if the signal from the amplifier output is to be transmitted over a greater distance, its higher amplitude will make it less sensitive to the electromagnetic interference and other noise sources. Second, if the input signal is amplified, then noise properties of the following stages are less critical [57]. It should be noted, however, that the gain of such a circuit must be selected according to the gain bandwidth product (*GBP*) of the operational amplifier and the required bandwidth of the signal. LMC662 has a typical *GBP* of 1.4 MHz, which

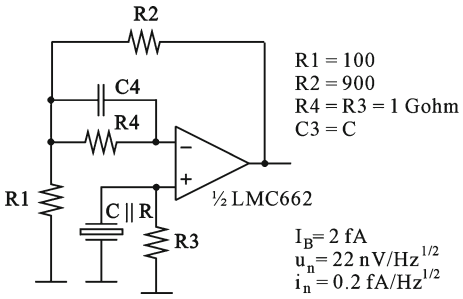

Fig. 5 Preamplifier for piezoelectric sensors working in the voltage mode (moderate bandwidth; gain of 10; single op-amp solution)

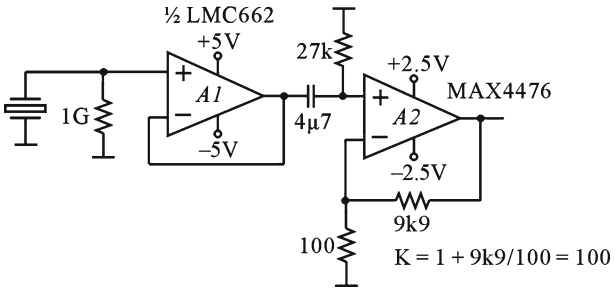

Fig. 6 Preamplifier for piezoelectric sensors working in the voltage mode (higher bandwidth; gain of 100; voltage follower with a subsequent amplifier stage)

means that if the feedback loop sets its gain to the value of approximately 10 as in Fig. 5, the signal bandwidth will be limited to only $GBP/K = 1.4$ MHz/10 = 140 kHz. Thus, if the bandwidth is of primary importance, the preamplifier should rather work in the configuration of a voltage follower, with a second stage based on an operational amplifier with a much lower noise voltage (taking into consideration that the noise adds with squares, an amplifier with a noise voltage of 20 % will increase the final noise by less than 5 %) and a much higher *GBP* (Fig. 6).

The $R4$ and $C4$ components ($R4 \approx R3$; $C4 \approx C$) in the circuit diagram from Fig. 5 are used to balance impedances at both amplifier inputs. Such a technique reduces the input offset voltage, because input bias currents of both inputs flow through similar resistances. Even more important is that such a solution also significantly decreases the output noise (Fig. 7). This results from the fact that in a FET input operational amplifier, the current noise of the bias circuitry can be coupled to the inputs via the gate-to-source capacitances and results in an additional input voltage noise component. However, taking into consideration that this noise component is correlated at both inputs, matching of the input impedances should reduce it substantially [54].

4.2 Charge Amplifier for Piezoelectric Sensors

In the charge amplifier configuration (Fig. 2b), a piezoelectric sensor is connected to the inverting input of the operational amplifier. Time variations of the charge produced by the sensor can be treated as the AC current component. Due to the virtual ground

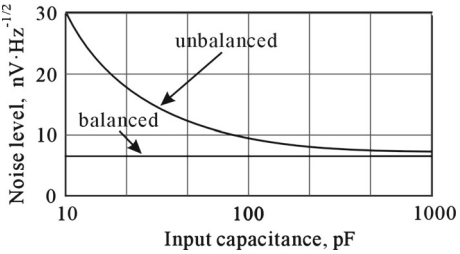

Fig. 7 Influence of unbalanced impedance of the operational amplifier inputs on the preamplifier noise [54]

(a potential close to zero, forced by the feedback loop of the amplifier) existing at the inverting input, dQ charge changes induced by the piezoelectric sensor causes a corresponding flow of current through the capacitor $C2$, producing d$Q/C2$ voltage at the output of the amplifier [38,52,54]. Similar to the previous case, the resistor $R2$ is required to supply bias current to the inverting input of the operational amplifier. In practical applications (Fig. 8), the non-inverting input is connected to the ground via a parallel connection of $R3$ and $C3$ (where $C3 = C1 \,||\, C2$, and $R3 = R1 \,||\, R2$) in order to balance impedances at both amplifier inputs. Parallel connections of $R1$, $C1$ and $R3$, $C3$ influence the frequency response of the charge amplifier, by determining lower f_{L} and upper f_{U} corner frequencies, respectively. Practical values of the upper cutoff frequency are usually below 100 kHz. Similarly, as in the voltage preamplifier, the operational amplifier should be a CMOS or JFET with the possibly lowest u_{n} noise value, but as the resistor values are usually much lower than in the case of the voltage amplifier, the input bias current I_{B} and current noise i_{n} values are much less critical. The operational amplifier used in the circuit presented in Fig. 8 is OPA192, for which typical specifications are $I_{\mathrm{B}} = 5$ pA, $u_{\mathrm{n}} = 5.5$ nV·Hz$^{-1/2}$, and $i_{\mathrm{n}} = 1.5$ fA·Hz$^{-1/2}$. Values of the resistors $R2$, $R3$ and capacitors $C2$, $C3$ are not given on the circuit diagram, because they depend on the characteristics of the sensor (mainly on its capacitance $C1$), as well as on the required signal gain and bandwidth.

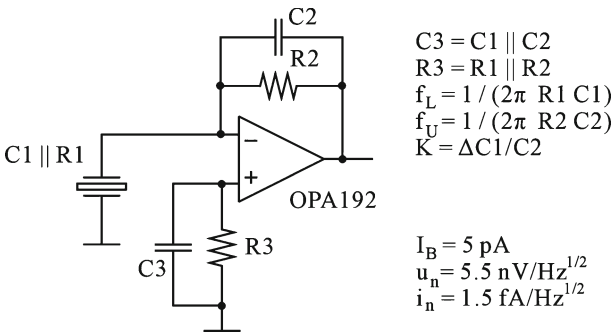

Fig. 8 Charge amplifier for piezoelectric sensors with balanced impedances at both operational amplifier inputs [54]

4.3 Measurement Condenser Microphone Preamplifier

Preamplifier circuits dedicated for externally polarized condenser microphones are usually implemented in voltage amplifier configurations, as in Fig. 2c [55]. The high-ohmic resistance $R1$ supplies DC polarization to the microphone, while the other high-ohmic resistor $R2$ is used to supply bias current to the operational amplifier. The main sources of noise in the circuit shown in Fig. 2c are resistors $R1$ and $R2$, and the amplifier A1. As previously discussed, from the point of view of the noise properties, $R1$ and $R2$ should be as large as possible. Unfortunately, resistances higher than 10 GΩ to 50 GΩ are not practical, because resistances $R1$ and $R2$ limit also the speed of charging the microphone and separating capacitance $C1$ to the polarization voltage after powering up the amplifier. A practical circuit that overcomes this problem is shown in Fig. 9 [56]. During measurements, both switches are opened, thus creating ultra-high resistance. They are closed for a short time before the measurements start in order to charge the separating capacitor $C1$ and the microphone to the polarization voltage. The resistors $R1$ and $R2$ connected in series with the switches are used to limit charging currents. Due to the extremely low input currents of the first stage amplifier and appropriate assembling, which minimize leakage currents, the DC operating point of the amplifier changes very slowly, so that the measurements can last minutes before the switches should be closed again [56]. The voltage at the output of LMC662 follows the microphone signal changes. The gain of the second stage of the preamplifier is fixed with resistors $R4$ and $R5$ ($K = 1 + R4/R5$). The capacitor $C2$ and the resistor $R3$ form a high-pass filter, which is used to remove a DC component from the MAX4488 input. The corner frequency of the filter $f_L = 1/(2\pi\, R3\, C2)$ can be selected according to the needs of a particular photoacoustic setup in which the preamplifier is used. At lower frequencies, noise characteristics of the circuit presented in Fig. 9 are substantially better than those of a commercial Bruel and Kjær 2669 condenser microphone preamplifier (Fig. 10) [56]. The main drawback of the circuit is the necessity of periodical closing of the switches. This problem can be

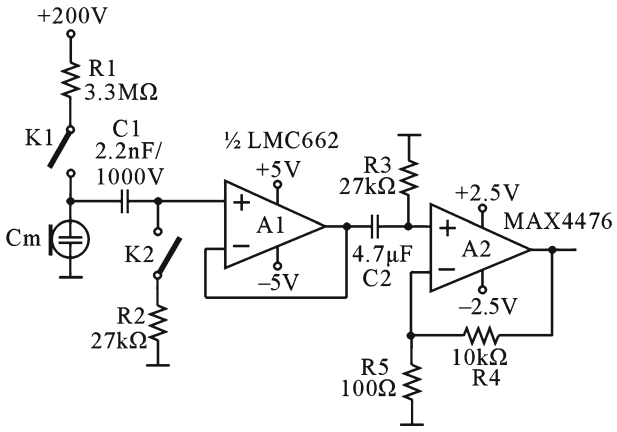

Fig. 9 Ultralow-noise preamplifier for measurement condenser microphones [56]

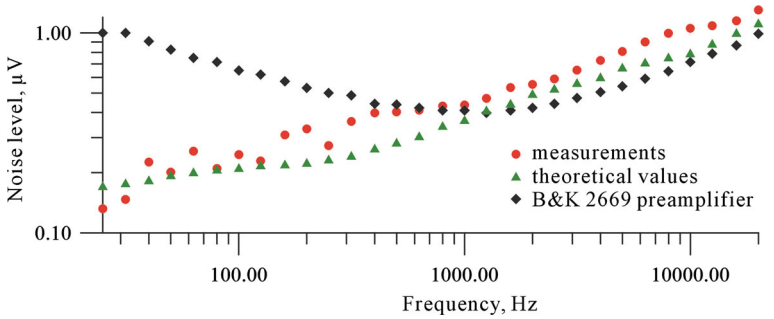

Fig. 10 Noise properties of the preamplifier from Fig. 9 [56]

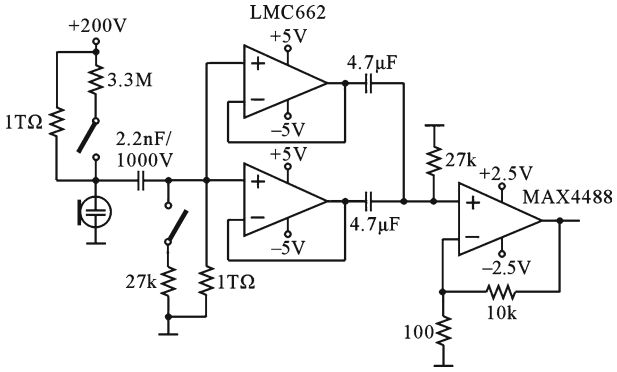

Fig. 11 Modified circuit of the preamplifier from Fig 9 resulting in further noise reduction and eliminating the need of periodical switching of the charging keys

solved by the use of additional ultra-high (1 TΩ) resistances, which compensate the operational amplifier input bias and leakage currents (Fig. 11). A parallel connection of two operational amplifiers results in noise averaging and reduces the output noise by approximately a factor of $1/\sqrt{2}$ [58]. Taking into consideration that the LMC662 contains two amplifiers in a single package, this noise reduction comes at no extra cost.

4.4 Measurement Electret (Pre-polarized) Microphone Preamplifier

In comparison to the condenser microphone preamplifier, a pre-polarized (electret) measurement microphone preamplifier can be substantially simplified, because there is no polarization voltage required. An example of such a circuit is given in Fig. 12. The resistor of 1 TΩ is used for supplying the bias circuit to the non-inverting input of the operational amplifier, and simultaneously removes from the microphone any unwanted charge which might otherwise lead to an erroneous sensitivity. It is clearly visible that the circuit is virtually the same as in the case of the piezoelectric sensor preamplifier working in the voltage mode (Fig. 2a).

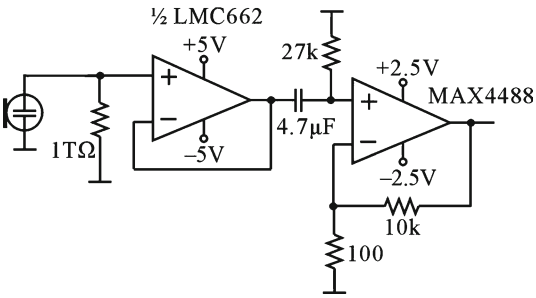

Fig. 12 Pre-polarized (electret) measurement microphone preamplifier

4.5 Low-Cost Electret and MEMS Microphone Preamplifier

Commercial MEMS microphones and low-cost electret microphones usually have an internal voltage follower or amplifier. Thus, their output is a low-impedance signal source, and there is no need for any external preamplifier dedicated for high-impedance transducers— outputs of such microphones can be directly connected to a standard amplification and filtering block that is described further.

5 General Structure of the Amplification and Filtering Block

The level of the photoacoustic signal obtained from the input sensor is usually low, especially in the case of trace concentration detection. However, the dynamic range of photoacoustic measurements can be very high—e.g., it can be easily noticed that implementation of concentration measurements ranging from single ppb to 1000 ppm requires a dynamic range of 120 dB. Some detectors, such as measurement microphones, allow for an even higher dynamic range. Getting such a high dynamic range directly in an analog-to-digital converter (at an acceptable signal-to-noise ratio and required sampling range) can be very difficult, if possible. It is usually much more convenient to enhance the dynamic range of the ADC with a programmable gain adjustment implemented in the analog signal path. Such a gain adjustment does not have to be very smooth- –switching the gain with binary or even decade steps is sufficient. Such a circuit can be implemented with existing integrated PGA (programmable gain amplifier) circuits—e.g., AD 8253, PGA 113, LTC 6912, etc. Every gain stage introduces a DC offset, which results from the fact that the input voltage offset of every stage is multiplied by its gain coefficient. As a result, even just 1 mV of the input voltage offset of an operational amplifier multiplied by the factor of $K = 10\,000$ should result in an output offset of 10 V, which in typical conditions would lead to saturation of the output amplifier. This is one of the reasons for which high gain factors (it should be mentioned that gains at the level of 10 000 are not unusual in photoacoustic setups) are usually implemented in several amplification stages (e.g., two PGAs). In order to reduce the offset, every gain stage should be AC coupled with the preceding circuit. This may be, in particular, implemented with a capacitor placed in the signal path or in a more complex high-pass filter.

Taking into consideration that the photoacoustic signal can be very weak (quite often it is buried in noise), filtering is a very important part of photoacoustic signal processing. An appropriately designed filter should pass only the frequencies of interest while rejecting (suppressing) other components of the input signal. As a result, the more narrow is the passband, the stronger will be the noise amplitude reduction. It should also be mentioned that low-pass sections not only limit the noise bandwidth, but also work as anti-aliasing filters, which must be used if the signal is to be subject to analog-to-digital conversion. The type of filter should be selected according to the particular application. If the shape of the photoacoustic pulse response is important, then a Bessel filter should be used. If the pulse response is not critical, but a flat frequency response in the passband is required, then a Butterworth filter should be used. Chebyshev and elliptic filters have a ripple in the pass band, but a steeper rolloff past the cutoff frequency [59,60]. Taking into consideration that any filter has a limited rolloff above its cutoff frequency, the filters are often cascaded in order to obtain stronger attenuation out of the passband [59]. A standard approach is that after every gain stage, a single- or double-zero/pole filter is placed. Thus, the resulting frequency response corresponds typically to a filter of at least second order, which is usually sufficient, as additional filtering (if needed) can be implemented as digital signal processing. Placing a filter after every gain stage allows for easy DC offset cancelation and reduces noise, giving more room for signal amplification without saturation of amplifiers. It might be tempting to use a programmable filter to get it more flexible and applicable in many applications. Such filters can be quite easily implemented as variable state filters with a multiplying DAC [61–63] or switched-capacitor filter. However, it should be noted that switched-capacitor filters are noisy [64], while the mentioned programmable variable state structure shows relatively poor attenuation properties [63]. Hence, it is usually better to use conventional analog filters with fixed cutoff frequencies selected according to a particular application.

6 ADC Selection Criteria

The primary selection criteria of the analog-to-digital converter are resolution and sampling rate. According to the Nyquist sampling theorem, it is sufficient to sample a signal with a frequency which is twice higher than the highest frequency component present in the signal spectrum to get correct information about the signal [65]. However, due to a strong increase of the anti-aliasing filter requirements, it is not recommended to obtain a sampling rate too close to the Nyquist frequency. Oversampling with a factor of at least 100 will substantially reduce these requirements. Moreover, a higher sampling rate improves the frequency resolution of the FFT (if applied to the recorded signal), and allows for averaging resulting in a better signal-to-noise ratio [65–67]. Hence, assuming that the photoacoustic signal will not contain components of interest above 10 kHz, a converter with a sampling rate at the level of 1 Msps should be sufficient. Now, taking into consideration that currently it is possible to buy a decent 16-bit ADC capable of working with a 1 Msps sampling rate for approximately $15, there is not much point in cutting the cost down to, for example, $5 for a 12-bit converter. Certainly, the sampling rate requirement depends strongly on the application and in particular on

the mode of operation of the designed photoacoustic system. If the system is to work in a pulse regime and the photoacoustic response to such pulses is to be recorded with a high time resolution, then, of course, higher sampling rates may be required.

7 Power Supply and Other Remarks

Measurement condenser microphones require a polarization voltage. A simple circuit that can be used to produce +200 V DC from a low supply voltage available locally is given in Fig. 13. V_IN can be of any value in the range of 3 V to 15 V. In order to reduce EMI noise resulting from switching, MAX1523 can be put in a shutdown mode for a few minutes (for the time of measurements) [68]. The output voltage can be precisely adjusted with potentiometer $R4$. If programmatic adjustment of the output voltage is required, then it can be implemented by replacing $R4$ with a digital potentiometer [68].

Power supply design may seem to be a simple task, but there are a few things that must be taken into account. One of the most important is the PSRR (power supply rejection ratio, which tells how much variations of the supply voltage are transferred to the signal path) of the components used in the front end. Certainly, the most critical is the PSRR of the first components in the signal chain, i.e., input sensor and preamplifier, because further front-end blocks work with the amplified signal. To give an example, if the PSRR is 60 dB and the supply voltage contains ripples of 1 mV, they will manifest in the signal path as an additional noise with an amplitude of 1 μV, which can be comparable to the photoacoustic signal level. The above example shows clearly that the PSRR of the critical parts should be really high, and for that reason, components such as the EK series microphones produced by Knowles, for which the PSRR is rated at a value of only 14 dB [69], should not be used in photoacoustic applications. Another conclusion is that the output of the analog power supply must be really clean—ultralow output noise linear regulators (e.g., TPS7A4700, LP38798, ADM7151, and ADM7160) are strongly recommended, while switching regulators should be avoided.

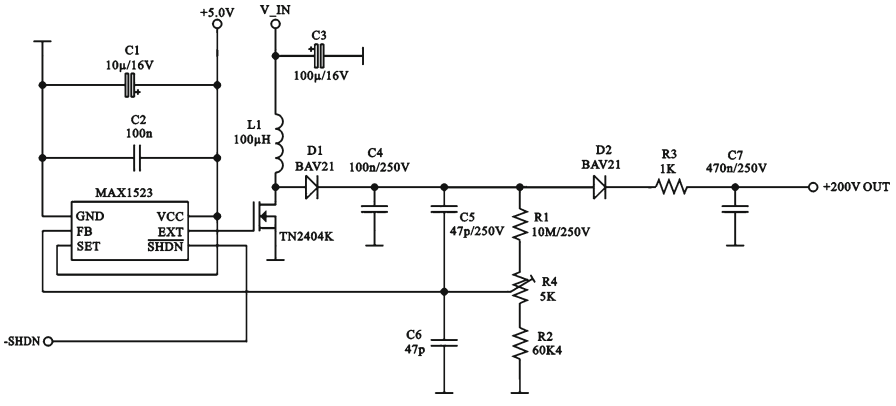

Fig. 13 Polarization voltage supply circuit for measurement condenser microphones

Appropriate decoupling and proper PCB design with a dedicated ground layer are also critical.

A very strong source of noise is 50 Hz electromagnetic interference (EMI). Taking into consideration that the input stages of the photoacoustic front end are very sensitive to any kind of EMI noise, shielding to prevent stray signal pickup and galvanic separation of the front end from the digital circuitry are strongly recommended [57]. In the case of very high-impedance preamplifier circuits, the surface leakage of the PC board must not be ignored. To minimize the effect of leakage, guard rings can be helpful [70–72], but for extremely low bias current applications (level of fA), all such connections should be made to a virgin Teflon standoff insulator [54]. After assembly, the board should be cleaned carefully and then sealed with a high-quality conformal coating material. Even better results can be obtained with point-to-point up-in-the-air wiring [72].

8 Conclusions

The design of analog front-end circuitry in piezoelectric or microphone detection of photoacoustic signals depends strongly on the type of the input sensor, application, and acceptable cost of the system. The first stage amplifier must work in a charge or voltage configuration. In any case, a low-noise and low EMI approach are critical. It is possible to design an analog front end for which the specification will be comparable with high-priced commercial solutions for a fraction of their costs (less than $100).

References

1. F.G.C. Bijnen, J. Reuss, F.J.M. Harren, Rev. Sci. Instrum. **67**, 2914 (1996)
2. V.A. Kapitanov, V. Zeninari, B. Parvitte, D. Courtois, Yu.N. Ponomarev, Spectrochim. Acta A **58**, 2397 (2002)
3. J. Davidsson, J.H. Gutow, R.N. Zare, J. Phys. Chem. **94**, 4069 (1990)
4. A. Petzold, R. Niessner, Appl. Phys. Lett. **66**, 1285 (1995)
5. E. Holthoff, J. Bender, P. Pellegrino, A. Fisher, Sensors **10**, 1986 (2010)
6. M.H. de Paula, A.A. de Carvalho, C.A. Vinha, N. Cella, H. Vargas, J. Appl. Phys. **64**, 3722 (1988)
7. J. Breguet, J.-P. Pellaux, N. Gisin, Proc. SPIE **2360**, 457 (1994)
8. S.L. Firebaugh, K.F. Jensen, M.A. Schmidt, J. Appl. Phys. **92**, 1555 (2002)
9. W. Jackson, N.M. Amer, J. Appl. Phys. **51**, 3343 (1981)
10. M.M. Farrow, R.K. Burnham, M. Auzanneau, S.L. Olsen, N. Purdie, E.M. Eyring, Appl. Opt. **17**, 1093 (1978)
11. N. Ledermann, P. Muralt, J. Baborowski, M. Forster, J.-P. Pellaux, J. Micromech. Microeng. **14**, 1650 (2004)
12. V.V. Kozhushko, G. Paltauf, H. Krenn, Acoust. Phys. **59**, 25 (2013)
13. A.A. Kosterev, YuA Bakhirkin, R.F. Curl, F.K. Tittel, Opt. Lett. **27**, 1902 (2002)
14. L. Dong, A.A. Kosterev, D. Thomazy, F.K. Tittel, Appl. Phys. B **100**, 627 (2010)
15. K. Liu, X. Guo, H. Yi, W. Chen, W. Zhang, X. Gao, Opt. Lett. **34**, 1594 (2009)
16. J. Fonsen, V. Koskinen, K. Roth, J. Kauppinen, Vibr. Spectr. **50**, 214 (2009)
17. K. Wilcken, J. Kauppinen, Appl. Spectr. **57**, 1087 (2003)

18. J. Kauppinen, K. Wilcken, I. Kauppinen, V. Koskinen, Microchem. J. **76**, 151 (2004)
19. S.M. Park, M.I. Khan, H.Z. Cheng, G.J. Diebold, Ultrasonics **29**, 63 (1991)
20. J. Hodgkinson, M. Johnson, J.P. Dakin, J. Appl. Phys. **98**, 084908 (2005)
21. S.J. Komorowski, E.M. Eyring, J. Appl. Phys. **62**, 3066 (1987)
22. K. Adelhelm, W. Faubel, H.J. Ache, Fresenius J. Anal. Chem. **338**, 259 (1990)
23. Q. Sun, C. Gao, B. Zhao, Y. Bi, Int. J. Thermophys. **31**, 1157 (2010)
24. I.V. Blonskij, V.A. Tkhoryk, M.L. Shendeleva, J. Appl. Phys. **79**, 3512 (1996)
25. J. Bodzenta, B. Pustelny, Z. Kleszczewski, Ultrasonics **31**, 315 (1993)
26. D.M. Todorović, M. Pawlak, I. Delgadillo-Holtfort, J. Pelzl, Eur. Phys. J. Spec. Top. **153**, 259 (2008)
27. T. Kitai, M. Torii, T. Sugie, S. Kanao, Y. Mikami, T. Shiina, M. Toi, Breast Cancer **21**, 146 (2014)
28. S. Manohar, S.E. Vaartjes, J.C.G. van Hespen, J.M. Klaase, F.M. van den Engh, W. Steenbergen, T.G. van Leeuwen, Opt. Expr. **15**, 12277 (2007)
29. S. Mallidi, T. Larson, J. Tam, P.P. Joshi, A. Karpiouk, K. Sokolov, S. Emelianov, Nano Lett. **9**, 2825 (2009)
30. S.I. Kudryashov, S.D. Allen, E.I. Galanzha, E. Galitovskaya, V.P. Zharov, Proc. SPIE **6086**, 60860J (2006)
31. V. Slezak, Appl. Phys. B **73**, 751 (2001)
32. G. Giubileo, F. Colao, A. Puiu, Laser Phys. **22**, 1033 (2012)
33. M.G. da Silva, H. Vargas, A. Miklós, P. Hess, Appl. Phys. B **78**, 677 (2004)
34. J.M. Rey, D. Marinov, D.E. Vogler, M.W. Sigrist, Appl. Phys. B **80**, 261 (2005)
35. E.M. Monahan Jr, A.W. Nolle, J. Appl. Phys. **48**, 3519 (1977)
36. O. Dóka, D. Bicanic, Photoacoustic spectrocopy: application in powdered biological samples. in *Proceedings of Forum Acusticum 2005* (Budapest, Hungary, 2005), pp. 1441–1446, ISBN 963 8241 68 3
37. J. Tichý, J. Erhart, E. Kittinger, J. Přívratská, *Fundamentals of Piezoelectric Sensorics*, chap. 1 (Springer-Verlag, Berlin, 2010)
38. G. Gautschi, *Piezoelectric Sensorics*, chap. 2 (Springer-Verlag, Berlin, 2002), p. 11
39. J. Dosch, B. Hynd, Analysis of electrical noise in piezoelectric sensors. Presented at Modal Analysis Conference, IMAC XXV: A Conference and Exposition on Structural Dynamics (Orlando, FL, 2007)
40. Condenser Microphone Cartridges—Types 4133 to 4181 (Brüel & Kjær, Naerum, Denmark), http://www.bksv.com/doc/Bp0100.pdf. Accessed 20 Apr 2014
41. GRAS, Selection Guide Microphones & Preamplifiers (G.R.A.S. Sound & Vibration A/S, Holte, Denmark), http://www.sagetechnologies.com/attachments/article/15/GRAS_Selection_Guide_Mics_Preamps_July_2011.pdf. Accessed 20 Apr 2014
42. Prepolarized Condenser Microphone Cartridges—Types 4129, 4155, 4176 (Brüel & Kjær, Naerum, Denmark), http://helmut-singer.de/pdf/bkua0308.pdf. Accessed 20 Apr 2014
43. Components Quick Guide (CUI Inc, Tualatin, OR, 2013) http://www.cui.com/catalog/resource/cui-component-quick-guide.pdf. Accessed 21 Apr 2014
44. Acoustic Interface Design Guide (Knowles, Itasca, IL, 2012), http://www.knowles.com/eng/content/download/4304/58695/version/7/file/Design_Guide.pdf. Accessed 21 Apr 2014
45. MEMS Microphone Devices (InvenSense Inc, San Jose, CA, 2014), http://www.invensense.com/mems/microphone/. Accessed 21 Apr 2014
46. AAC Technologies, Global Leading Micro-Component Total Solution Provider, http://www.aactechnologies.com/category/10. Accessed 21 Apr 2014
47. Akustica, Bosch Group, Akustica MEMS Microphones, http://www.akustica.com/microphones.asp. Accessed 21 Apr 2014
48. MEMS Microphones (Wolfson Microelectronics, Santa Clara, CA, 2014), http://www.wolfsonmicro.com/products/mems-microphones/. Accessed 21 Apr 2014
49. H. Bruhns, A. Marianovich, M. Wolff, Int. J. Thermophys. (2014). doi:10.1007/s10765-014-1690-5
50. M. Pedersen, J. McClelland, Proc. SPIE **5732**, 108 (2005)
51. W.Q. Liu, Z.H. Feng, R.B. Liu, J. Zhang, Rev. Sci. Instrum. **78**, 125107 (2007)
52. J. Karki, *Signal Conditioning Piezoelectric Sensors*, Application Report SLOA033A (Texas Instruments, Dallas, 2000)
53. V. Sharapov, *Piezoceramic Sensors*, chap. 4 (Springer-Verlag, Berlin, 2011)
54. J.S. Wilson, *Sensor Technology Handbook*, chap. 4 (Elsevier, Amsterdam, 2005)
55. Microphone Handbook, vol. 1: Theory, chap. 2–4 (Brüel & Kjær, Naerum, Denmark, 1996), http://www.bksv.dk/doc/be1447.pdf. Accessed 21 Apr 2014

56. T. Starecki, Rev. Sci. Instrum. **81**, 124702 (2010)
57. H.W. Ott, *Electromagnetic Compatibility Engineering*, chap. 8–9 (Wiley, Hoboken, 2009)
58. J. Williams, *Composite Amplifiers*, Application Note 21 AN21-12 (Linear Technology, Milpitas, 1986)
59. J. Karki, *Active Low-Pass Filter Design*, Application Report, SLOA049 (Rev, B) (Texas Instruments, Dallas, 2002)
60. R. Mancini, *Op Amps for Everyone*, chap. 16, Design Ref. SLOD006 (Rev. B) (Texas Instruments, Dallas, 2002)
61. Circuit Applications of Multiplying CMOS D to A Converters, Application Note AN-269, (National Semiconductor, Santa Clara, CA, 1981)
62. AD7628: CMOS Dual 8-Bit Buffered Multiplying DAC, AD7628 Data Sheet (Analog Devices Inc, Norwood, MA, 1996)
63. T. Starecki, M. Grajda, Proc. SPIE **6347**, 63471G (2006)
64. K. Lacanette, *A Basic Introduction to Filters—Active, Passive, and Switched-Capacitor*, Application Note AN-779 (National Semiconductor, Santa Clara, CA, 1991)
65. AVR121: Enhancing ADC Resolution by Oversampling, Application Note AVR121, (Atmel, San Jose, CA, 2005)
66. Improving ADC Resolution by Oversampling and Averaging, Application Note AN018 (Cygnal, Austin, TX, 2001)
67. T. Starecki, Proc. SPIE **6159**, 61592N (2006)
68. T. Starecki, Proc. SPIE **6347**, 63471H (2006)
69. EK Series, Electret Condenser Microphone Datasheet (Knowles, Itasca), http://media.digikey.com/pdf/Data%20Sheets/Knowles%20Acoustics%20PDFs/EK%20Series.pdf. Accessed 21 Apr 2014
70. K. Blake, *Op Amp Precision Design: PCB Layout Techniques*, Application Note AN1258, (Microchip, Chandler, AZ, 2012), http://ww1.microchip.com/downloads/en/AppNotes/01258B.pdf. Accessed 21 Apr 2014
71. R.J. Widlar, *Working with High Impedance Op Amps*, Application Note AN-241 (National Semiconductor, Santa Clara, CA, 1980)
72. LMC662: CMOS Dual Operational Amplifier (datasheet) (National Semiconductor, Santa Clara, CA, 2003)